Chapter 2

Theoretical Background

2.1 Basics of Magnetic Energies

Understanding the magnetic ground state of the system is possible with basic theoretical background knowledge. The basics of magnetism that can help to understand the physically significant terms are discussed in this chapter. Here, a brief introduction to the exchange interaction, especially superexchange, is discussed. Along with the exchange interaction, magnetization dynamics using the Landau-Lifshitz- Gilbert equation will be touched to give an overview of the magnetic dynamics in ferrimagnetic systems. After stating the equation, its term for the dissipation of magnetic energy has also been briefly discussed. Magnetic materials possess spontaneous magnetization, which makes them promising in various applications like memory, computation, compass, etc. To better understand, it is essential to investigate the properties' fundamentals. This chapter focuses on a perspective that helps build a basic foundation on various significant aspects.

2.1.1 Exchange Energy

The Weiss molecular field [52] theory could not explain the reason behind the ferromagnetic state of transition metals. After that, in 1928, Heisenberg proposed the Hamiltonian for the ferromagnetic state [53]. Considering the example of the hydrogen molecule, Heisenberg explained the ground state using a quantum mechanical approach. He considered two Hydrogen atoms and the resultant wavefunction (Ψ) has been calculated by combining spatial (ϕ) and spin (χ) wavefunctions. $\Psi = \phi\chi$. The final Ψ has to be antisymmetric. For spatially symmetric wave function, the spin wavefunction has to be antisymmetric and vice versa. The probability of an asymmetric spatial wavefunction suggests the localization of electrons around the separate atoms, and the probability of a symmetric wavefunction suggests the sharing of electrons by both atoms equally. He stated that the two identical electrons can be exchanged between the two hydrogen nuclei. This interaction between exchangeable electrons was termed an "exchange interaction." The Hamiltonian for Heisenberg exchange interaction has been expressed as follows:

$$H = -2\sum_{i<j}^{N} J_{ij}\hat{S_1}.\hat{S_2} \tag{2.1}$$

where J is exchange integral, $\hat{S_1}$ and $\hat{S_2}$ spin vectors of atom 1 and 2, respectively. The value of J decides whether spins will be aligned parallel or anti-parallel. Figure (2.1): depicts the wavefunction and probability density in the hydrogen molecule

The equation for exchange integral (J) is as follows:

$$J = \frac{E_S - E_T}{2} \tag{2.2}$$

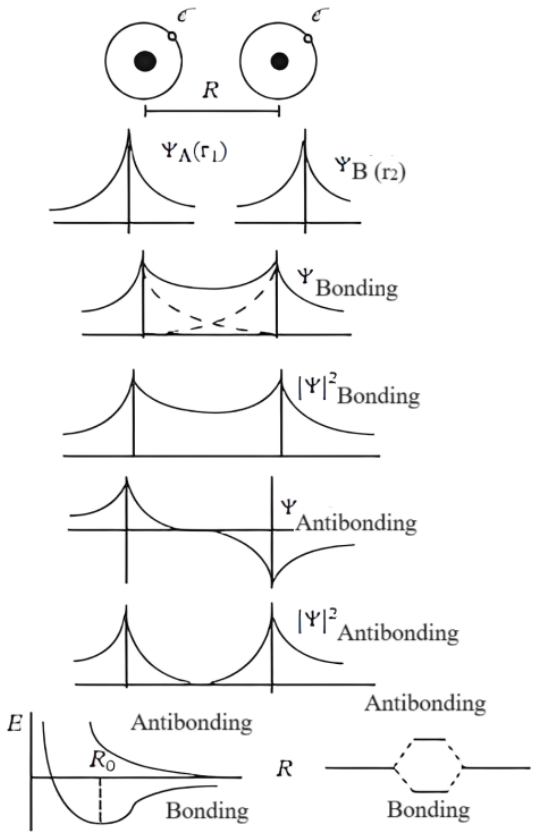

Fig. 2.1 *The interaction between two hydrogen atoms based on bonding and anti-bonding of the wavefunctions. Figure adapted from [15].*

where E_S is the energy of the singlet spin state, and E_T is the energy of the triplet spin states. If E_S is lower, then J is negative, which means it is an antiferromagnetic ground state, and if E_T is lower, J is positive and supports a ferromagnetic ground state.

There are broadly two exchange interactions, i.e., direct and indirect. When the two magnetic species interact directly without the intermediate species, known as direct interaction, for example, $Co_{23}Fe_{11}Cu_{66}$, $Co_xFe_yB_z$. When nonmagnetic species like oxygen or electrons mediate the exchange interaction, it is known as an indirect exchange interaction. The indirect exchange that happens in the electron gas is known as Ruderman-Kittel-Kasuya-Yoshida (RKKY) interaction [54] and the oxygen intermediated exchange between two

similar species is known as superexchange if it happens between two different cationic states is known as the double exchange [55]. An asymmetric exchange known as the Dzyloshinskii-Moriya interaction gives rise to exciting spin textures. Iron garnets show the superexchange kind of indirect exchange interaction. Superexchange is explained in detail as follows.

Superexchange energy

Metals have free electrons, making studying the underlying exchange interaction difficult. In the case of transition metal oxides, covalent bonding is present, which facilitates localized electrons and helps in studying the magnetic order. Taking the example of MnO, oxygen-mediated superexchange interaction is shown. The oxygen (O^{2-}) ion (electronic configuration, [Ne]) in an electronically full-filled state intermediating the two half-filled Mn^{2+} cations (electronic configuration, [Ar]$3d^5$]), which further shows an antiferromagnetic coupling, as depicted in Figure: (2.2) that shows how p_z orbital of O^{2-} overlap with the Mn^{2+} cation orbitals [15, 56, 57, 58].

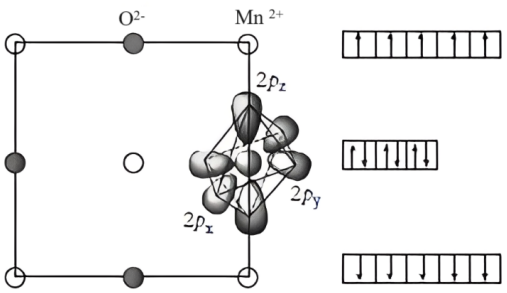

Fig. 2.2 *Orbital structure of linearly coupled Mn^{2+} and O^{2-} cation in Mn^{2+}-O^{2-}-Mn^{2+} configuration in MnO. Electron configuration of 3d and 2p orbitals, coupled using antiferromagnetic superexchange interaction, adopted from [15].*

This intermediated indirect exchange among similar species of cations is known as the superexchange. It can be antiferromagnetic or ferromagnetic, depending on the electronic

state of the valence electrons. Based on the two fundamentals of quantum physics, Pauli's exclusive principle and Hund's rule, a set of rules for the superexchange interaction is known as the Goodenough-Kanamori rules. It describes superexchange interaction as antiferromagnetic when the virtual electron transfer is between two half-filled orbitals [59]. In contrast, superexchange interaction changes into a ferromagnetic nature when it is between half-filled to empty orbitals or filled to half-filled orbitals [59].

In iron garnets the Fe^{3+} cations interact with the mediating O^{2-} anions, similar to the Mn^{2+} and O^{2-} interactions. As per the Goodenough-Kanamori rule, the half-filled d-orbital of Fe^{3+} cations are antiferromagnetically coupled. This antiferromagnetically coupled competing tetrahedral and octahedral species of the Fe cations gives rise to an uncompensated moment in the formula unit and results in the ferrimagnetic ordering in the iron garnets.

2.1.2 Magnetic Anisotropy

The scalar Heisenberg interaction shows isotropic exchange in the ferromagnets, antiferromagnets, and ferrimagnets [15]. In reality, the magnetization is anisotropic. This anisotropy could be because of the sample's crystallographical axes, stress, and shape [57]. Anisotropy seems like an issue to the uniform magnetization, but it plays an important role in the domain wall width, stabilizing the exotic spin textures, designing the actuators and motors, Hard-drive disk, and sensors [60, 61]. In this section, the overview of the different magnetic anisotropy is as follows:

Magneto-crystalline anisotropy

The magnetization of the magnetic system is dependent on its crystallographic axis. This anisotropy in magnetization due to the crystallographic axis is known as magneto-crystalline anisotropy [62]. This arises due to spin-orbit coupling (SOC) in the material.

Due to the crystal field, orbitals affect the spin orientations; this asymmetry gives rise to magneto-crystalline anisotropy. Iron garnets have a combination of uniaxial and cubic magnetocrystalline anisotropy. The axis along which the magnetization saturates at a low magnetic field is the easy axis, and the highest magnetic field required to saturate the magnetization is the hard axis. In cubic crystals, magnetic anisotropy is known as cubic magneto-crystalline anisotropy. Let α_1= cos a, α_2 = cos b, and α_3 = cos c be directional cosine of magnetization vectors. The anisotropy energy density of the cubic crystals is as follows:

$$E_{mc} = K_0 + K_1(\alpha_1^2\alpha_2^2 + \alpha_2^2\alpha_3^2 + \alpha_3^2\alpha_1^2) + K_2\alpha_1^2\alpha_2^2\alpha_1^2 + ... \tag{2.3}$$

Where K_0, K_1, and K_2 are the different order contributions of the anisotropy constant at a certain temperature. The higher-order constant has been neglected here. In this case, K_2 is very small and, therefore, can neglect it. As the K_0 term has nonangular dependence and we only see the difference in the anisotropy energy here, it has been neglected. For both YIG and TmIG is K_1 is -1.1 $\times 10^3$ N/m^2 [63, 64].

Stress-induced anisotropy

A thin film is grown over a single crystal substrate. The interface constrains the lattice parameter of the grown thin film. This asymmetry breaks the symmetry of the grown thin film. The lattice mismatch between the bulk and interface gives rise to stress in the thin film and the anisotropy originates, hence it is termed as stress -induced anisotropy. The magnetic energy variation arises from the strain in a system known as magnetostriction and the associated energy is magnetoelastic energy. In this dissertation, the sample has been grown along the <111> orientation; therefore, stress-induced anisotropy is along the <111> direction and can be written in an equation as follows:

$$K_\sigma = -\frac{3}{2}\lambda_{111}\sigma \tag{2.4}$$

where, K_σ is stress-induced anisotropy constant, λ_{111} is magnetostriction constant along <111> crystallographic axis, and σ is stress in the direction. λ_{111} values for YIG and TmIG are -1.7 $\times 10^{-6}$ and -5.2 $\times 10^{-6}$, respectively [65, 66]. The stress-induced anisotropy significantly contributes to the epitaxial iron garnet thin films. In TmIG, lattice mismatch causes perpendicular magnetic anisotropy in the deposited thin films.

Shape anisotropy

The internal field present inside the material opposes the magnetization of the magnetic materials, which depends on the material' geometry. The magnitude and direction of the magnetization also depend on the geometry; for example, in a needle, the easy magnetization direction is along the length because shape anisotropy is weaker in that direction. This energy is also known as shape anisotropy, demagnetization field, and magnetostatic energy. Figure: (2.3) showing the magnetic lines of the field of (a) H field and (b) B field in a bar magnet. The middle notation shows B and 4πM are parallel, and H_d (demagnetization field) is anti-parallel to them. As demagnetization energy opposes the magnetization of the magnetic materials, it is applied internally, unlike a stray field.

The energy equation for the demagnetization is as follows:

$$E_{demagnetization}/Volume = \mu_0 \int_0^M H_d.dM(SI) \tag{2.5}$$

H_d can calculated by using the equation:

$$H_d = -N_d.M \tag{2.6}$$

N_d is a demagnetization tensor (dimensionless) depending on the geometry of the sample, and M is magnetization. Here, equation (2.6) shows that the demagnetization field is the

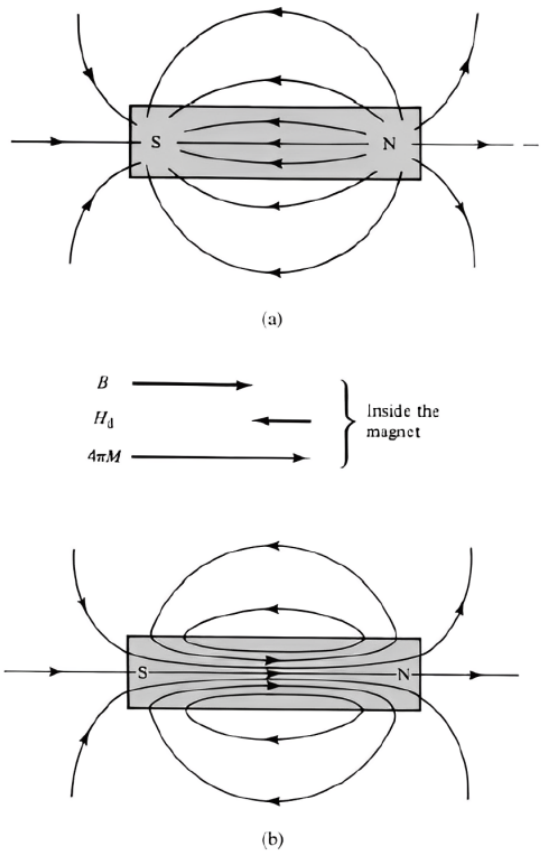

Fig. 2.3 *Field lines of a bar magnet without external field. (a) H field, and (b) B field. Middle arrows shows the direction of the B, H_d (demagnetization field) and $4\pi M$ at the center of the bar magnet adapted by [57].*

opposite of the magnetization of the magnetic matter. The E_d decreases with the formation of the domain walls.

Iron garnets have a perfect cubic crystal structure, and magnetizing them in the different orientations of the crystal symmetry needs different energy, bringing about cubic magnetocrystalline anisotropy. The thin film is a two-dimensional system, and the thicker relaxed film shows the easy magnetization direction in the XY plane. This dissertation shows the stress-induced uniaxial anisotropy (the out-of-plane magnetization), which results in the perpendicular magnetic anisotropy in the TmIG.

2.1.3 Zeeman Energy

Pauli's exclusion principle states that no two electrons can occupy the same quantum number state in an atom. Electrons have four quantum numbers: principle quantum number (n), azimuthal quantum number (l), magnetic quantum number (m_l), and spin quantum number (m_s). The value of l lies 0,1,2,...,n-1 and m_l vary from -l,....-1,0,1,....l. The value of m_s is $\pm \frac{1}{2}$. The magnetic quantum number is degenerated without an external magnetic field. Application of external field breaks this degeneracy as presented in Figure (2.4).

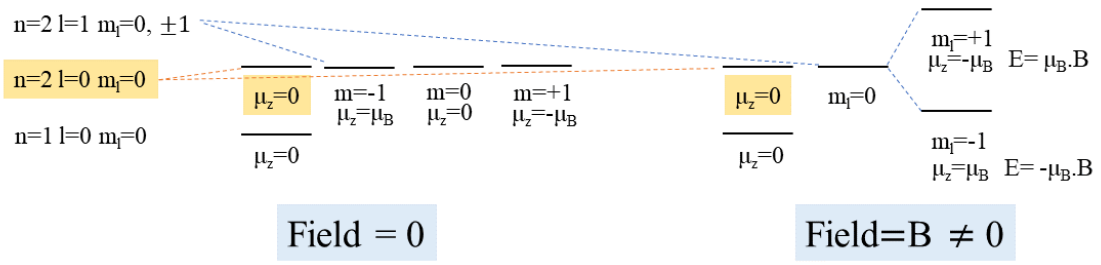

Fig. 2.4 *Energy level splitting in the absence (presence) of an applied external magnetic field.*

Take an example of $l = 1$ state, which is a three-fold degenerate state (m_l = 0, ±1) that breaks into three different energy states with energy -μ_BB, 0, and +μ_BB. This phenomenon of non-degeneracy is known as the "Zeeman effect" [15, 56, 57]. These split energy levels absorb the energy of microwave frequencies and show resonance. This resonance probes the magnetic properties of the sample. FMR is a spectroscopy technique based on this resonance.

2.2 Magnetization dynamics

FMR works on the principle of FMR, which occurs when the frequencies of the magnetization precession around the effective magnetic field resonate with an externally applied microwave frequency. It is a time-dependent field causing the precession due to exposing the matter to GHz frequency waves, which shows resonance at that field. The magnetic external field at which resonance occurs is the resonance field. The energy losses happen with the precession within the time duration of tens of nanoseconds. These energy losses give rise to the linewidth in the resonance spectra. The Landau-Lifshitz equation is a mathematical way to understand the precession of magnetization and relaxation of the magnetization vector, which was further edited by Gilbert, and the final equation known as the Landau-Lifshitz-Gilbert equation. This equation and its terms have been elaborated in next section.

2.2.1 The Landau-Lifshitz-Gilbert Equation

Considering all the magnetic energies explained briefly in this chapter, in 1935 Landau and Lifshitz derived a dynamical magnetization equation, incorporating relativistic interactions in the relaxation term. This form of magnetization dynamics is known as the Landau and Lifshitz equation (LL) [67]. Furthermore, a useful form of the damping term was derived by modifying the LL equation done by Gilbert in 1954 [68]. Collective work of Landau, Lifshitz, and Gilbert on the magnetization dynamics equation, known as the Landau-Lifshitz-Gilbert equation (LLG). It exhibits the various nonlinear magnetic states, namely skyrmions, spin waves, and elliptical function waves [69]. LLG equation is as follows:

$$\frac{dM}{dt} = \gamma[M \times H_{eff}] - \alpha[M \times \frac{dM}{dt}] \tag{2.7}$$

where, γ is gyromagnetic ratio, α is the Gilbert damping constant, and H_{eff} is effective magnetic field. Figure (2.5) (a) shows the precession of magnetization around an effective magnetic field, and (b) shows the damping of the amplitude due to Gilbert damping. The magnetization vector precesses around the direction of effective magnetic field and is damped to the equilibrium with the applied field. Here, the direction of magnetization changes, but the magnitude remains constant. Therefore, inelastic magnon scattering is not involved. More details about the Gilbert Damping is explained in the next section. Before discussing the damping parameter, the next section of derivation presents the resonance condition for the FMR and gives the idea of how, under different energies, resonance happens and its derivation by the LLG equation.

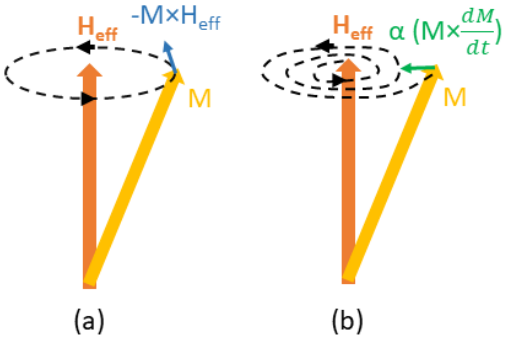

Fig. 2.5 *Schematics of (a) Magnetization (M) precession and (b) damping (α) of precession around an effective magnetic field (H_{eff}).*

2.3 Magnetization damping

Understanding the relaxation of the magnetic systems is necessary because of their importance in spin wave propagation and spin pumping. The magnitude of the relaxation should be small to give an easy flow to the spin waves that depends on the intrinsic and extrinsic properties of the system. It is also called damping. The linewidth in FMR is the result of these relaxations. Landau and Lifshitz introduced the damping concept in their magnetic

dynamics equation, presenting the damping term λ in the 1930s [67]. Gilbert further modified it in the 1950s and termed it the famous α, the term of Gilbert damping [68]. This simplification, or the more significant term, is adopted by the research community to explain the experimental determination of the fastest propagator of the spin waves, iron garnets [70]. This section presents the significance of the damping terms and explains the broad division of the intrinsic and extrinsic damping terms. These intrinsic and extrinsic dampings are also known as the Gilbert and non-Gilbert damping, respectively, based on their origin. Intrinsic factors like electron interactions and SOC affects the damping and give the Gilbert damping. The nonhomogeneous contribution due to magnon-magnon scattering and the defects gives rise to the non-Gilbert damping in magnetic systems.

Experimentally, this can be calculated by plotting the linewidth as a function of the frequency; both intrinsic and extrinsic contributions can be separated as represented by the following equation:

$$\Delta H = \Delta H_0 + \frac{4\pi\alpha}{\gamma} f \tag{2.8}$$

where, ΔH is linewidth, ΔH_0 is an inhomogeneous contribution to the linewidth, α is the intrinsic Gilbert damping parameter, and f is the resonant frequency. In this section, both intrinsic and extrinsic contributions have been discussed in detail.

2.3.1 Intrinsic Damping

The magnetically ordered materials' intrinsic properties affect the relaxation of spin excitation. Initially, the origin of the Landau-Lifshitz (LL) damping coefficient was studied by Kamberskỹ in the 1970s [71]. The LL damping coefficient calculation by Kamberskỹ was done using the low-frequency approximation in linear response theory. This theory applies well to the itinerant model with relatively short-lived quasistationary electron states [71]. It states that due to the SOC, perturbation in the magnetization

magnitude and direction prompts a non-equilibrium population state seen as the Fermi state's deviation or breathing known as the Kamberskỹ to the equilibrium state. The model given by the Kamberskỹ is known as the breathing Fermi-surface model [72]. Because of the perturbation induced by the SOC, the energies of the Bloch states depend on the magnetization direction. As the direction of the magnetization change with the excitation, there will be a small change in the Fermi surface (stated as breathing of the Fermi surface), resulting in the relaxation of the population of density of states to the actual equilibrium state. The relaxation happens when the Bloch states close to the Fermi surface transfer its energy to the lattice vibrations. In simple words, as the spin is not conserved while deriving λ, the conclusion was that the origin lies in the SOC, and the restricted conservation of the spin results in the angular momentum transfer to the lattice, which results in the damping [73]. This was the explanation for the LL damping parameter. The Gilbert damping parameter study was performed with further advancement in the relativistic Dirac equation.

In 2009, Hickey et al. presented the first-principles calculation for the α, modifying the relativistic Dirac equation to the nonrelativistic Dirac equation with the SOC perturbation in magnetically ordered materials [74]. This study first considers a relativistic Dirac particle, solving the Dirac-Pauli Hamiltonian by the Foldy-Wouthuysen transformation. Get the results in the Zeeman, spin-orbital, and Darwin terms. The time-dependent part of the Hamiltonian is examined further, and the rate equation governs the time evolution of the magnetization observable in the non-equilibrium regime. This term is rewritten in the LLG equation, resulting in the value determination of the α. The first principle calculations have proven the α is as follows:

$$\alpha = \frac{ie\hbar\mu_0 M_S}{8m_0^2c^2}(1-\chi_m^{-1}) \tag{2.9}$$

where, $\hbar$ is the reduced Planks constant, M_s is the saturation magnetization, m_0 is the rest mass, c is the speed of light in vacuum, and χ_m is magnetic susceptibility. α has intrinsic properties, and this dissertation studies this property to evaluate the quality of the deposited thin films. The smaller the α, the more cycles are needed for magnetization to stabilize. YIG is the lowest reported α material.

As the spin precession propagates, spin accumulates in the heavy metal as the spin current if the ferro/ferrimagnetic layer has topped with the heavy metal with a high SOC. This pumping of spin in the thin film of heavy metal from the ferromagnetic magnetic layer is similar to the adiabatic charge pumping in the mesoscopic systems, known as spin pumping. This phenomenon was proposed by Silsbee et al. in 1979 [75]. They studied the angle-dependent FMR of the ferromagnetic/nonmagnetic interfaces and observed the phase of the magnetic susceptibility changes with the angle, and there they concluded the resonance creates a transverse magnetization in the surrounding, known as spin pumping. However, as the various magnetic/nonmagnetic interfaces were studied, the results showed that the spin pumping also gave rise to the Gilbert damping parameter. The spin accumulation in the nonmagnetic layers generates a backward flow of the spin current to the ferromagnetic layer, and these interacting spin currents affect the LLG equation, which enhances the Gilbert damping parameter [76, 77]. This spin current generation has spintronics and quantum gates applications [78, 79].

2.3.2 Extrinsic Damping

The inhomogeneous extrinsic contribution to the linewidth comes from defects of the magnetic system that break translation symmetry. ΔH_0 is the inhomogeneous contribution to the linewidth in equation (2.8). A major mechanism for the non-Gilbert damping is two-magnon scattering [80, 81, 82, 25]. Initially, the role of voids and porous in the nearly ideal single crystal of YIG was studied by Spark-Loudon-Kittel in 1961 [83]. The defects,

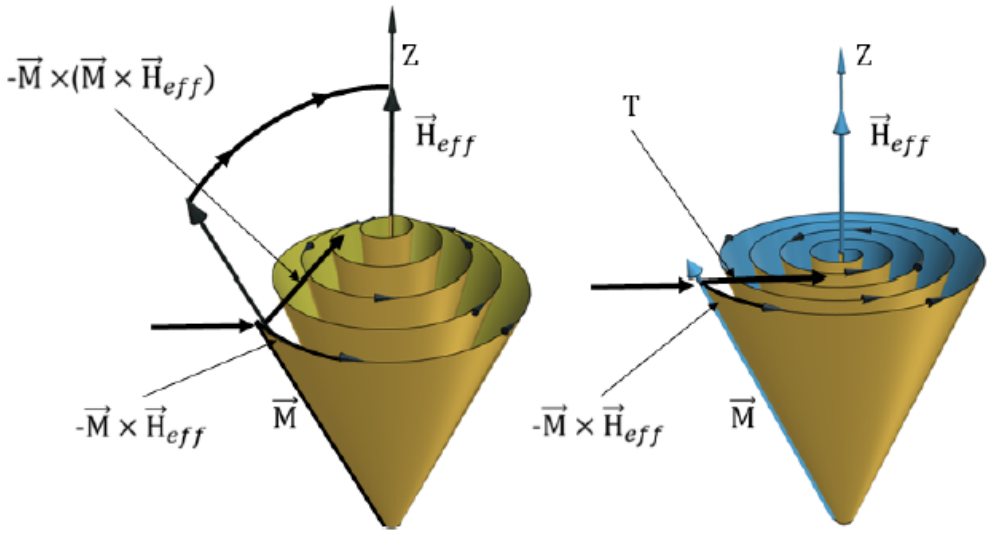

Fig. 2.6 *Left is the Landau-Lifshitz model of the magnetization precession and the right schematic of Bloch–Bloembergen (BB) gyromagnetic process adopted from [84].*

dislocations, impurities, surface roughness, thin film thickness, lattice mismatch due to strain, and consequently, magnetic property variations because of all these contribute to extrinsic damping [84]. Similar to the LLG equation, another approach to understanding the magnetic precession and damping was given by Bloch and Bloembergen [85, 86]. This equation gives the signature of the spin-spin relation in the process of the damping. The Bloch-Bloembergen (BB) equation explains the two-magnon scattering by considering the z-vector of the magnetization remains constant as presented in Figure (2.6). The BB equation is given below [[84]]:

$$\frac{\delta M}{\delta t} = -\gamma(M \times H_{eff}) - \frac{M_x}{T_2}\hat{e}_x - \frac{M_y}{T_2}\hat{e}_y - \frac{M_z - M}{T_1}\hat{e}_z \tag{2.10}$$

where, M is magnetization, T_1 is longitudinal relaxation time, T_2 is transversal relaxation time, and $\hat{e}_{x,y,z}$ as the unit directions in coordinate axis. The BB equation considers the net magnetization of the system, opposite of the LLG, where individual magnetic moments are studied. The two relaxations in the BB equation are for both the spin waves' uniform and nonuniform excitation modes, which are direct and indirect, respectively. The BB equation

gives the linewidth considering T_2 is as given below:

$$\Delta H = \frac{\delta H_{res}}{\delta \omega_0} \frac{1}{T_2} \tag{2.11}$$

where, H_{res} is resonance magnetic field. The linewidth is a consequence of the transverse relaxation process (spin-spin relaxation). This relaxation presents the two-magnon scattering effect on the damping of the magnetization. In conclusion, this linewidth is inhomogeneous extrinsic damping due to the lack of an ideal crystal structure or the continuity of it that causes magnetic perturbation in the system. This work observes high extrinsic damping because of the grain boundaries in the polycrystalline thin films and surface and interfacial roughness and strain in the epitaxial thin films.